MICROSTRUCTURE STABILITY AND CREEP BEHAVIOUR OF ADVANCED HIGH CHROMIUM FERRITIC STEELS

VÁCLAV SKLENIČKA[1]* , KVĚTA KUCHAŘOVÁ[1], JIŘÍ KUDRMAN[2], MILAN SVOBODA[1], LUBOŠ KLOC[1]

[1] *Institute of Physics of Materials, Academy of Sciences of the Czech Republic, Žižkova 22, CZ-616 62 Brno, Czech Republic*
[2] *UJP PRAHA, a.s., Nad Kamínkou 1345, CZ-156 10 Prague-Zbraslav, Czech Republic*

Received 22 October 2004, accepted 16 December 2004

The creep resistance of two high chromium ferritic power plant steels (grades P91 and P92) is shown to be considerably influenced by microstructure changes and microstructure stability during long-term isothermal annealing and/or creep over a range of dislocation (power-law) creep. It is suggested that the change in the dislocation substructure is much more important than the indirect effect caused by particle evolution. By contrast, no significant effect of microstructure stability on creep was found in a regime of viscous creep that is inherent to real service loading conditions of the steels of interest. Finally, no deterioration of the creep properties was found for the steels P91 and P92 under cyclic creep (nonsteady stressing and heating) in a regime of power-law creep.

K e y w o r d s: 9–12%Cr steels, microstructure stability, creep behaviour, nonsteady creep loading

1. Introduction

The efficiency of conventional boiler/steam turbine fossil power plants is a strong function of the steam temperature and pressure. The need to reduce CO_2 emission recently provided an additional incentive to increase efficiently. Thus, steam temperatures of the most efficient fossil power plants are now in the 600 ℃ range and it is expected that temperatures will rise in the very near future [1–3].

The main enabling technology is the development of stronger high temperature materials. Worldwide research has resulted in a number of new 9–12%Cr steels with improved creep strength [1–5]. Optimization of C, Nb, Mo, and V and partial

*corresponding author, e-mail: sklen@ipm.cz

substitution of W for Mo in the 9–12%Cr steels have resulted in two steels (P91 and P92), capable of operating up to 620 ℃ at steam pressures up to 34 MPa. However, for the long-term application of the new steels, it is necessary to assess the microstructure changes that are likely to occur during service exposure and to evaluate the effect of such changes on the high-temperature creep behaviour. Only with this information designed values for components can be correctly assigned.

Although the development and evaluation of 9–12%Cr steels have proceeded on the basis of simple short-term laboratory-type tests, it is widely recognized that the realistic application of these materials is under conditions far different from those for which they were developed. When applied in service, the material is likely to be subjected to periods of removal of load, temperature, or both. Periodic applications of excessive loads and temperatures are normally absent when the steel is evaluated. Thus the further object of the present paper is an attempt to obtain some information on the effects of nonsteady stressing and heating on the creep properties of P91 and P92 steels.

The first part of this paper deals with the experimental investigation of the effect of long-term isothermal annealing on creep behaviour of P91 and P92 steels. Its second part deals with the effect of cyclic thermal loading on creep of P91 and P92 steels to simulate the operating regime which has many cycles of heating/cooling.

2. Experimental materials and procedures

The P91 material, a tempered martensitic-ferritic steel produced by Vitkovice Steel, Czech Republic, was subjected to the two-stage heat treatment: 1060 ℃/1 h/air + 750 ℃/2 h/air. Its chemical composition (in wt.%): 0.09 C, 0.56 Mn, 0.20 Si, 0.021 P, 0.009 S, 0.05 Cu, 0.46 Ni, 8.36 Cr, 0.86 Mo, 0.20 V, 0.06 Nb, 0.065 N and 0.007 Al. The P92 material was produced by Nippon Steel, Japan received in the form of a seamless pipe with the following heat treatment: 1065 ℃/2 h/air + 770 ℃/2 h/air. Its chemical analysis (in wt.%): 0.08 C, 9.0 Cr, 0.5 Mo, 1.8 W, 0.2 V, 0.06 Nb, 0.05 N, 0.003 B, $<$ 0.04 Al. Both P91 and P92 steels were investigated both in the as-received state (i.e. after standard heat treatment) and after isothermal annealing at 650 ℃ for 10000 hours to simulate long-term service conditions.

Standard constant load tensile creep tests were carried out at 600 ℃, using applied stresses ranging from 100 to 350 MPa. All of the tensile creep specimens were run to final fracture. Sophisticated short-term creep tests were performed on P91 steel at 600 ℃ and at low stresses below 100 MPa by means of the helicoidal spring specimens technique [6–8].

The effect of temperature variation during the creep exposure has been investigated by intermittent heating cycles in which the creep specimen was alternately held at the creep testing temperature for predetermined periods of time and then cooled down to room temperature ($\sim$ 144 h at 600 ℃, and $\sim$ 24 h at room tem-

perature, respectively). In all cases the load (tensile stress) was maintained during the entire test.

Following creep testing, samples were prepared for examination by transmission and scanning electron microscopy. Observations were performed using Philips CM 12 STEM and Philips SEM 505 microscopes.

3. Experimental results

3.1 The effect of long-term isothermal ageing on the creep behaviour of P91 and P92 steels

3.1.1 Creep results

In order to accelerate some microstructure changes and thus to simulate long--term service conditions, isothermal ageing at 650 ℃ for 10000 h was applied to P91 and P92 steels in their as-received states in an effort to obtain a more complete description of the role of microstructure stability in high-temperature creep of these steels.

Figures 1 and 2 show selected creep curves for steel P91 and steel P92 for uniaxial tensile creep tests conducted at 600 ℃ under the same level of the applied stress σ. As demonstrated by the figures, significant differences were found in the creep behaviour of both steels in the as-received state when compared with their behaviour after ageing. First, the standard ε vs. t curves (Figs. 1 and 2) appear to show that long-term isothermal ageing of the steels leads to an increase in the

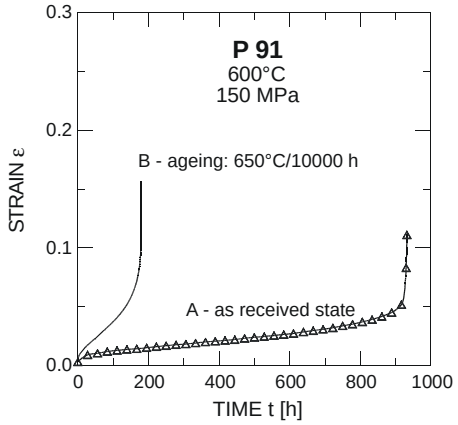

Fig. 1. Creep curves of the P91 steel in the as-received state and after long-term ageing (600 ℃, 150 MPa).

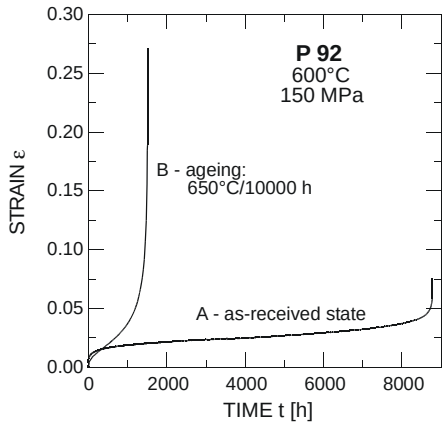

Fig. 2. Creep curves of the P92 steel in the as-received state and after long-term ageing (600 ℃, 150 MPa).

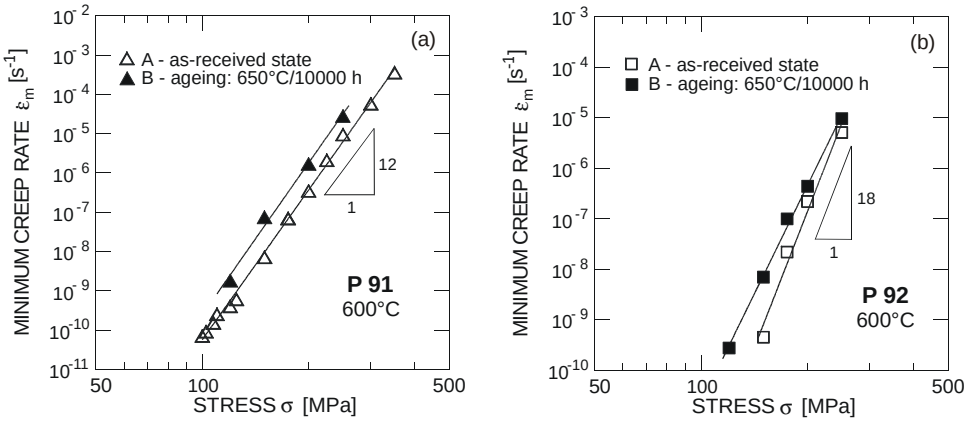

Fig. 3. Stress dependences of minimum creep rate for (a) P91 and (b) P92 steels.

creep plasticity, which is proved, in particular, by the value of the total strain to fracture for the aged P92 steel (Fig. 2). Second, the aged steels exhibit markedly shorter times to fracture than the steels in the as-received state. Third, the shapes of creep curves for both the as-received state and aged state of the steels differ considerably.

In Fig. 3, the minimum creep rates $\dot{\varepsilon}_{\mathrm{m}}$ are plotted against the applied stress σ on a logarithmic scale. Inspection of Fig. 3 leads to two observations. First, the steels in the as-received state exhibit better creep resistance than those after long--term ageing over the entire stress range used; the minimum creep rate for steel P91 in the as-received state is about order of magnitude less than that of the aged P91 steel. The stress dependences of the minimum creep rates for steel P92 are different in trend. While the slope and therefore the stress exponents of creep rate $n = (\partial \ln \dot{\varepsilon}_{\mathrm{m}}/\partial \ln \sigma)_{\mathrm{T}}$ are the same for steel P91 (Fig. 3a), the slope and the stress exponent n for steel P92 depend on its state; the difference in $\dot{\varepsilon}_{\mathrm{m}}$ between as-received and aged state increases with decreasing applied stress (Fig. 3b). For both steels, the double logarithmic plots of the time to fracture t_{f} as a function of applied stress are shown in Fig. 4. It is clear from these plots that the creep life of steels in the as-received state is longer than in the aged steels. While the difference for steel P91 is independent of applied stress, for steel P92 this difference consistently decreases with increasing applied stress, with a tendency at the higher stresses towards no effect of the state of steel on the lifetime.

Creep testing by means of the helicoidal spring specimens was performed at the applied stress ranging from 1 to 100 MPa and at 600 ℃ on steel P91 in both the as-received and aged states (Fig. 5). Inspection of this Figure suggests that

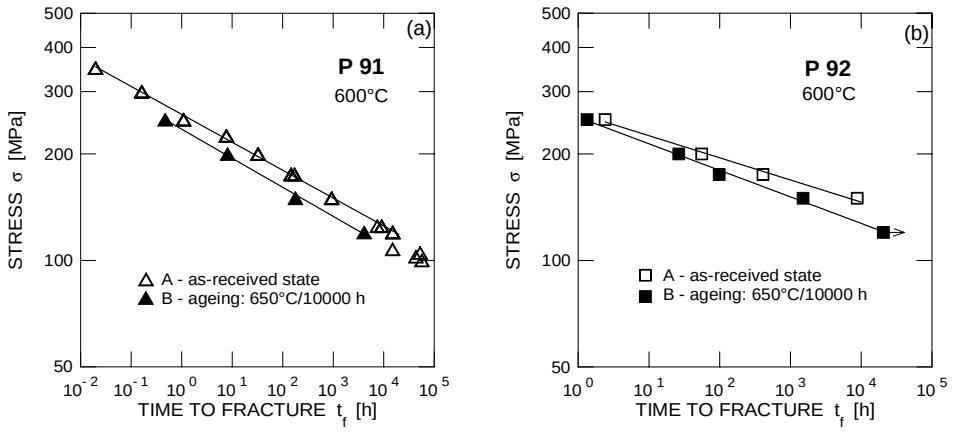

Fig. 4. Stress dependences of the time to fracture for (a) P91 and (b) P92 steels.

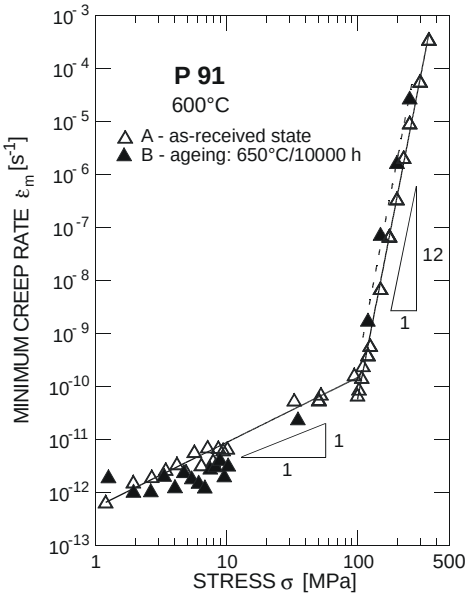

Fig. 5. Stress dependences of minimum creep rate for P91 steel in both power-law ($\sigma \geq 100$ MPa) and viscous ($\sigma \leq 100$ MPa) creep regimes obtained by a standard creep testing ($\sigma \geq 100$ MPa) and by the helicoidal spring creep specimens testing ($\sigma \leq 100$ MPa).

the minimum creep rates are proportional to applied stress up to about 100 MPa ($n \cong 1$). Mutual comparison of the creep results obtained by the helicoidal spring specimen technique with the results of standard uniaxial tensile creep tests on the steel investigated has shown very good coherency of both creep testing techniques. The transition from power-law creep (dislocation creep) with the stress exponent

of the creep rate n of about 12 to the viscous creep ($n = 1$) was found at stresses around 100 MPa at 600 ℃ (Fig. 5). It should be emphasized that any extrapolation from the power-law creep regime to stresses below 100 MPa may lead to serious underestimation of the creep rate predicted. No substantial effect of long-term ageing was found for the viscous creep. The creep rate for the aged state seems to be slightly lower than those for the as-received state.

3.1.2 Microstructural investigations

Microstructure of P91 steel is documented in Fig. 6. There are tiny precipitates of minor phase, present both on grain boundaries and on former martensitic laths in as-received state (Fig. 6a). Isothermal annealing at 650 ℃ for 10000 h leads to substantial coarsening of secondary phases particles on boundaries. Careful examination revealed also an increase of very small particles inside the former martensitic laths (Fig. 6b). The similar situation was found out also for P92 steel, see micrographs in Fig. 7. Nevertheless, stereological analysis of the crept specimens has revealed substantial difference between these two steels, mainly in the number of particles in volume unit after the creep exposure at 600 ℃, as can be seen in Fig. 8. The isothermal annealing prior to creep test did not have any significant effect on the number of particles in volume unit in P91 steel, as shown in Fig. 8a. By contrast, noticeable difference between the numbers of particles in volume unit for P92 steel was found in as-received and annealed state, as shown in Fig. 8b.

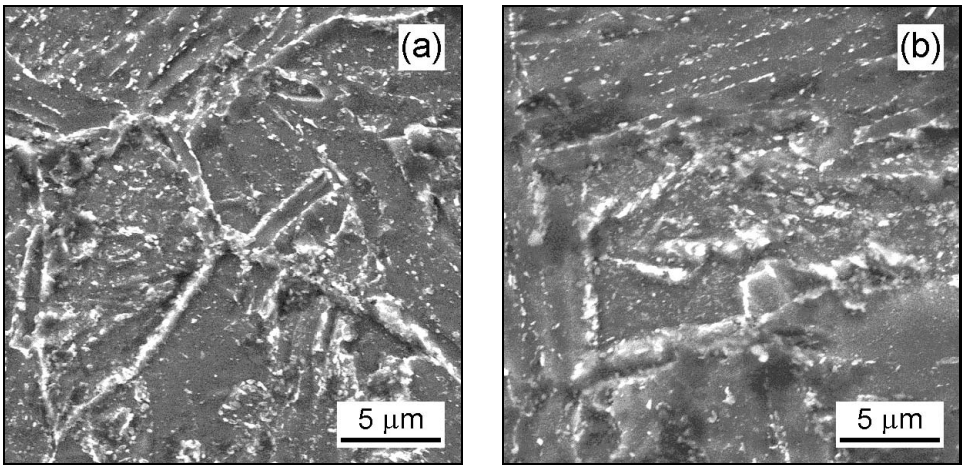

Fig. 6. SEM micrographs showing microstructure of P91 steel: (a) in as-received state and (b) after ageing at 650 ℃ for 10000 h.

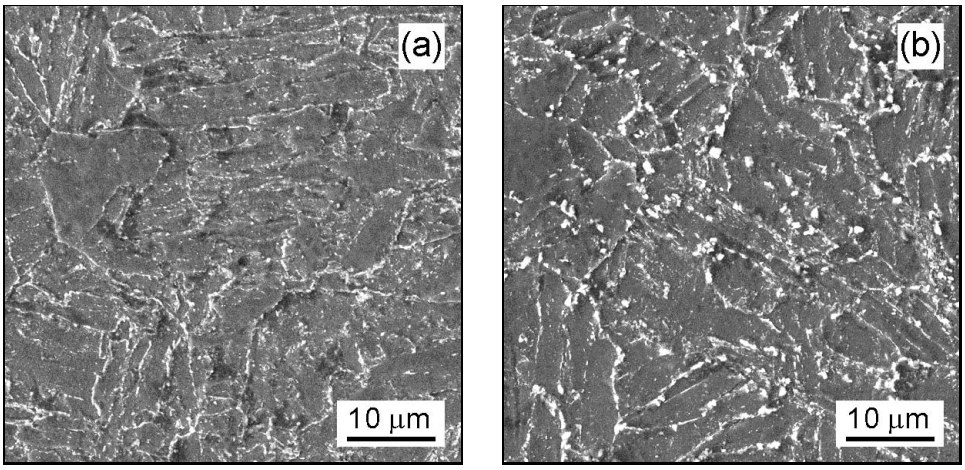

Fig. 7. SEM micrographs showing microstructure of P92 steel: (a) in as-received state, and (b) after ageing at 650 °C for 10000 h.

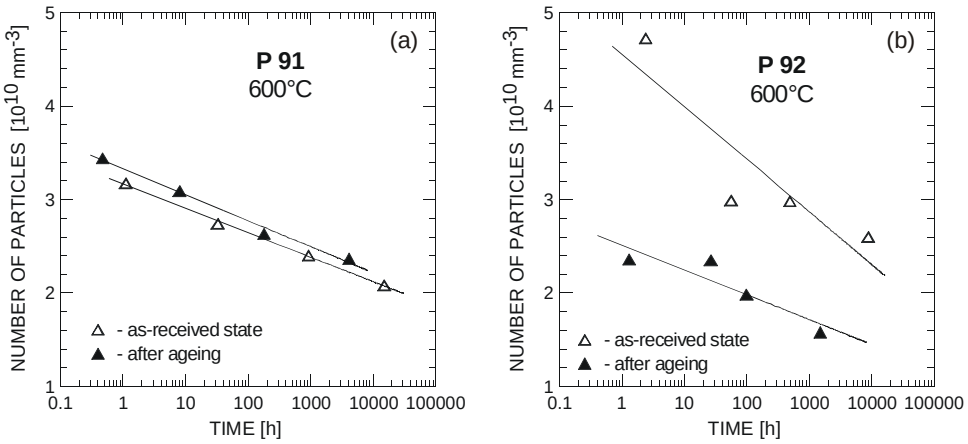

Fig. 8. Time dependences of the volume density of particles for steels P91 and P92 creep at 600 °C: in (a) as-received state, and (b) after ageing at 650 °C for 10000 h.

3.2 The effect of nonsteady loading in creep

Critical high temperature components of machines and structures are often subjected to complicated load and temperature histories. The closest laboratory simulation should involve both the temperature and stress cycles. For example, the

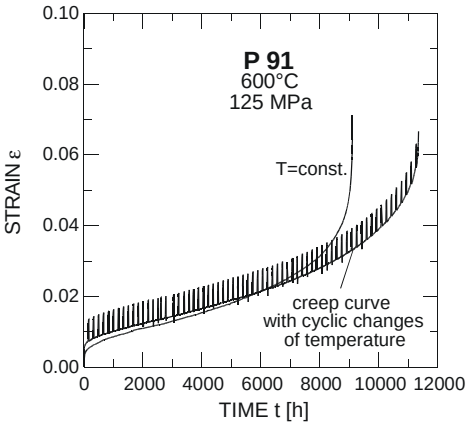

Fig. 9. Creep curves of the steel P91 with different loading histories in power-law creep regime.

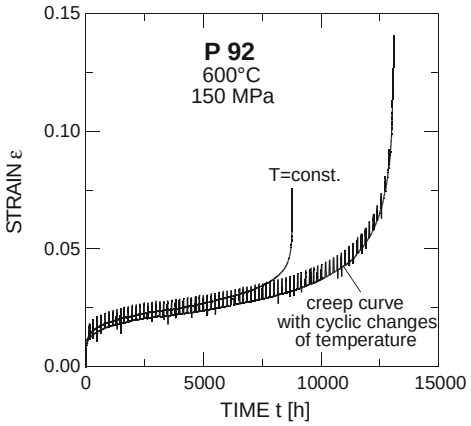

Fig. 10. Creep curves of the steel P92 with different loading histories in power-law creep regime.

start up and shut down cycles can be well simulated by temperature cycling with or without hold times. Another type of nonsteady stressing is the isothermal loading with stress cycling. In order to consider the above effects of different loading, one needs to design experimental methods for simulating the operating state which has many cycles of heating/cooling and nonsteady stressing.

In following temperature-cycled tests, the specimens in one cycle were moved first from room temperature to 600 ℃, then creep loaded (the holding time after stabilization of the temperature was 144 hours) and finally the specimens were cooled under load down to room temperature. This cycle was repeated from the beginning of the creep test up to the final fracture of specimen. Two creep curves with different loading history for steel P91 are shown in Fig. 9 in the form of strain ε versus time t for the testing temperature of 600 ℃ and under the same level of the applied stress of 125 MPa. The first curve represents an uninterrupted creep test which was run to the final fracture at constant testing temperature. The second curve shows the creep behaviour of specimen with cycled temperature loading which was fractured after 66 cycles. The similar creep curves of steel P92 are shown in Fig. 10 for the same testing temperature and the applied stress of 150 MPa. In this case, the cycled specimen was fractured after 77 cycles.

As demonstrated by the figures, no significant differences were found in the creep behaviour between the cycled tests and the uninterrupted ones. The cycled specimens exhibit a little longer creep life than the uninterrupted specimens. A possible explanation for this difference in creep life may lie in a serial addition of holding and cooling periods for a cycled specimen. In fact, the time to fracture

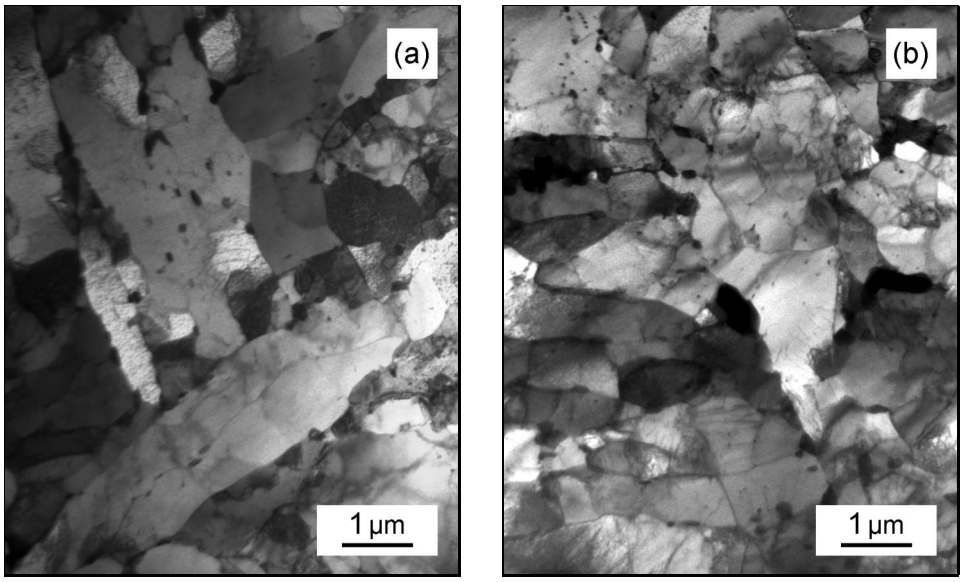

Fig. 11. TEM micrographs of P91 steel subjected to (a) monotonic and (b) cyclic creep (600 °C, 125 MPa).

for an uninterrupted specimen of P91 steel is about 9000 h whereas the test piece endurance for a cycled specimen is ∼ 9500 h when derived from holding periods only. Thus, it is clear from these experiments that the creep lives of steels P91 and P92 are not deteriorated by nonsteady heating.

The microstructures of specimens subjected to both the monotonic and the nonsteady creep loading are very similar (Fig. 11) and exhibit an evolution that can be described by the following phenomena: (i) rearrangement and annihilation of excess transformation dislocations; the dislocation density decreases; (ii) equiaxed subgrains develop from the former tempered martensite structure. Dimensions of newly formed subgrains are finer in comparison to the former tempered martensite laths; (iii) the interparticle spacing and the sizes of carbides $M_{23}C_6$ and fine particles MX increase.

4. Discussion

A power plant may have a life of 40 years. If a total creep strain of 1 pct is permissible, the average creep rate is about 10^{-11} s^{-1}. Extrapolation to this rate from rates measurable in the standard laboratory creep testing is perilous (Fig. 5), and we need to understand the physical processes involved. At these low rates of creep deformation, the transport of matter occurs by migration of vacancies rather

than by the glide of dislocations. These creep processes are usually classified as viscous creep [3, 4]. Viscous creep can proceed by Nabarro-Herring [9] and/or Coble diffusion creep [10], or by Harper-Dorn creep [11]. The existence and theoretical interpretation of viscous creep in pure metals are well established [12]; by contrast, the understanding of viscous creep in materials hardened by precipitates is very incomplete at present.

At the lower stresses in Fig. 5, the experimental points appear to lie along a line having a slope of $n = 1$. It can be shown theoretically that there is a value of $n = 1$ for all viscous mechanisms. Thus, the low stress region of $n = 1$ in Fig. 5 can be attributed to viscous creep. However, it is less easy to distinguish experimentally between various types of creep giving the same value of n. The main difference between them is in the grain size dependence of the creep rate [12]. Since the steel P91 tested was only one grain size, no creep mechanisms identification is possible.

Although no coherent explanation of the creep behaviour of the P91 steel in the low stress region can be given along the lines discussed above, it can be concluded that no significant effect of microstructure stability on creep behaviour may be expected at low strain rates where diffusion creep and/or Harper-Dorn creep dominates.

To determine the rate-controlling process(es) in creep in the high stress region ($\sigma \geq 100$ MPa), the slopes in the plots of the minimum creep rates vs. stress were determined at 600 ℃ for both P91 and P92 steel in the as-received and aged states (Fig. 3a,b and Fig. 5). The stress dependence of the creep rate can be described by an equation of the power-law form:

$$\dot{\varepsilon}_{\min} \propto A\sigma^n, \tag{1}$$

where A and n are constants at a given temperature. The evaluated high stress exponent $n \gg 1$ indicates the presence of the power-law or dislocation creep [12]. The stress exponent n changes from 12 (steel P91, Figs. 3a and 5) to 18 (steel P92, Fig. 3b).

Fig. 4 shows the stress dependence of the time to fracture t_f. Here again the straight-line approximation shows a good fit to the data, providing that the power--law relationship of the type

$$t_f \propto B\sigma^{-m} \tag{2}$$

is obeyed. The evaluated values of the stress exponent m are very similar to the values for stress exponent n. This can be explained by the fact that both the creep deformation and fracture are controlled by the same mechanism.

At present we are still at some distance from a more complete description and understanding of significant microstructural features and deformation mechanisms responsible for the enhanced creep strength of tempered martensite ferritic

9–12%Cr steels in dislocation (power-law) creep. The movement of dislocations through the matrix is at first resisted by (a) the dislocation substructure distribution (dislocation strengthening mechanism), (b) intragranular particles, mainly MX (particle strengthening), and (c) the strain fields associated with elements in solid solution (solid solution strengthening). As creep progresses the dislocation substructure changes to form subgrains whose boundaries are stabilized by $M_{23}C_6$ and MX particles and possibly also by Laves phases [5]. However, as these particles form and coarsen they denude the surrounding matrix of elements in solid solution, thus reducing the contribution of solid solution strengthening to creep resistance. Thus it seems likely that, as these changes progress, creep resistance becomes less and less dependent on resistance to the movement of individual dislocations through the matrix and more and more dependent on the resistance to subgrain growth through boundary migration.

Recently, Sklenička et al. [13], Čadek et al. [14] and Orlová et al. [15] reported extensive studies and analyses of creep behaviour and microstructure of the P91 steel in the region of the power-law creep. The analyses suggested strongly that: (i) the creep rate is not recovery controlled, (ii) neither is the creep rate controlled by dislocation climb around carbide particles provided no interaction of dislocations with a carbide particle takes place; and finally (iii) the Rösler-Arzt model [16] assuming an attractive interaction of dislocations with dispersed particles and thermally activated detachment of the dislocations from the particles, failed to account for the creep data of the P91. A metallographic analysis had shown that the effect of the rearrangement of dislocations and subgrain coarsening on creep may be more important than the effect of precipitation strengthening [13–15]. However, some evidence has been found for suppression or retardation of subgrain boundaries by the particles. A similar conclusion has also been convincingly demonstrated by Kuchařová et al. [17] using a novel approach in which creep specimens of P91 steel (in the as-received state) were subjected to additional thermo-mechanical treatments to change the subgrain and particle structures.

The contributions of the various microstructural features (dislocation density, subgrain size, carbide, carbonitride, and intermetallic precipitates) to the creep strength of P92 steel have been extensively studied. Ennis [18] reported that in P92 steel, during the first 3000 h of exposure at 600–650 ℃, a rapid reduction in the dislocation density and increase in size of $M_{23}C_6$ precipitates occur. The fine carbides, nitrides, and carbonitrides are stable and do not coarsen significantly. Decreasing of the dislocation density before testing by high temperature tempering reduces the creep strength. If the martensitic transformation is suppressed by appropriate heat treatment, P92 steel exhibits very low creep strength. Hattestrand and Andren [19] studied an isothermally aged P92 and found that coarsening of $M_{23}C_6$ carbides is accelerated by the strain, while the effect of strain on VN precipitates is insignificant. According to these authors, MX (mainly VN) precipitates appear

to be relatively stable during ageing for up to 10000 h at 600 and 650 °C. With $M_{23}C_6$ precipitates the situation is different. At 600 °C, no coarsening appears to take place during 10000 h of ageing, while in creep the particles coarsen to about 20 % larger size. At 650 °C, particle coarsening takes place in both aged and creep tested material. The role of tungsten (P92 steel has the addition of 1.8 wt.% tungsten in comparison with P91 steel) was studied by Hald [20]. It was found that W enters precipitates as intermetallic Laves phase during creep exposure, but the loss of tungsten from solid solution does not seem to affect long-term creep stability. Subgrains in steel P92 grow as a function of creep strain and stress following a general function for all 9–12%Cr steels, which indicates that the precipitate stability may control the creep strength of the steels. While MX (VN) particles coarsen very slowly during creep exposure, precipitation of new MX particles during creep could not be confirmed.

From the above discussion, it can be concluded that the creep behaviour and the creep strength in the power-law creep region are controlled by the coexistence of dislocation substructure and precipitates, the latter mainly acting as subgrain stabilizer. Thus, the role of dislocation substructure dominates the role of precipitation strengthening due to carbide particles. Consequently, a decrease of the creep resistance of the aged steels may be explained by taking account of the change of dislocation substructure during isothermal ageing.

Interpretation of the detailed creep behaviour following non-steady loading is not straightforward but several unambiguous conclusions can be drawn. They should be based on the state of material, containing internal distribution of all microstructural elements, stress and strain. Since any of the state parameters may have its own kinetics depending on all other parameters, the solution of the problem is very difficult. It is important to realize that there is no physical reason for conclusion, that every state of the material can be reached by simple loading history, like the combined constant stress – constant temperature test.

The temperature changes consisting in cooling the specimen from the testing temperature of 600 °C down to the room temperature and heating up again to the testing temperature may cause some additional strain generated by the thermal stresses created during temperature changes. However, this phenomenon seems to have no substantial effect on the creep behaviour of the specimen. Provided that the microstructures of specimens subjected to both monotonic and cyclic loading are very similar, there is no reason for different creep behaviour of uninterrupted and cycled creep specimens.

5. Conclusions

The creep resistance of two modified 9–12%Cr steels (grades P91 and P92) at 600 °C is shown to be considerably influenced by microstructure changes during long-term ageing at 650 °C for 10000 h and/or creep over a range of dislocation

(power-law) creep. Significant differences were found in the creep behaviour of both steels in the as-received state when compared with their behaviour after ageing. Long-term isothermal ageing of the steels leads to an increase in the creep plasticity, however, the aged steels exhibit markedly shorter times to fracture than the steels in the as-received state. It is suggested that the creep behaviour and the creep strength in the power-law creep regime are controlled by the coexistence of dislocation substructure and precipitates, the latter mainly acting as subgrain stabilizer. Thus, the role of dislocation substructure dominates the role of precipitation strengthening due to carbide particles. Consequently, a decrease of the creep resistance of the aged steels may be explained by taking account of the change of dislocation substructure during isothermal ageing. By contrast, no significant effect of microstructure stability on creep was found in a regime of viscous creep at very low stresses.

No significant deterioration of the creep properties was found for the steels P91 and P92 under temperature-cycled creep loading in power-law creep. Provided that the microstructures of specimens subjected to both monotonic and cyclic loading are very similar there is no reason for different creep behaviour of uninterrupted and cycled creep specimens in a regime of power-law creep.

Acknowledgements

Financial support for this work was provided by the Czech Science Foundation under Grant No. 106/02/0608 (power-law creep experiments) and by the Academy of Sciences of the Czech Republic under Grants IQS200410502 and A2041101 (viscous creep experiments).

REFERENCES

[1] FUJITA, T.: In: Proceedings of the 3rd Conference on Advances in Material Technology for Fossil Power Plant. Eds.: Wiswanathan, R., Bakker, W. T., Parker, J. D. Swansea, The Institute of Materials 2001, p. 33.
[2] KERN, T.-U.—STAUBLI, M.—MAYER, K.-H.—ESCHER, K.—ZEILER, G.: In: Proceedings of the Int. Conference on Materials for Advanced Power Engineering. Eds.: Lecomte-Becker, J. et al. Forschungszentrum Jülich 2002, p. 1049.
[3] STAUBLI, M.—MAYER, K.-H.—GISELBRECHT, W.—STIEF, J.—DI GIAFRANCESCO, A.—KERN, T. U.: ibid, p. 1065.
[4] ABE, F.—IGARASHI, M.—WANIKAWA, S.—TABUCHI, M.—ITAKAGI, T.—KIMURA, K.—YAMAGUCHI, K.: In: Proceedings 3rd EPRI Conference on Advances in Materials Technology for Fossil Power Plants. Swansea, The Institute of Materials 2001, p. 79.
[5] SKLENIČKA, V.—KUCHAŘOVÁ, K.—SVOBODA, M.—KLOC, L.—BURŠÍK, J. —KROUPA, A.: Materials Characterization, *51*, 2003, p. 35.
[6] BURTON, B.—GREENWOOD, G. W.: Met. Sci. J., *4*, 1970, p. 215.
[7] KLOC, L.—FIALA, J.—ČADEK, J.: Mater. Sci. Eng., *A 130*, 1990, p. 61.
[8] KLOC, L.—SKLENIČKA, V.: Mater. Sci. Eng., *A234–236*, 1997, p. 962.
[9] NABARRO, F. R. N.: Metal. Mater. Trans., *33A*, 2002, p. 213.

[10] COBLE, R. L.: J. Appl. Phys., *34*, 1963, p. 1679.
[11] HARPER, J.—DORN, J. E.: Acta Metall., *5*, 1957, p. 654.
[12] ČADEK, J.: Creep in Metallic Materials. Amsterdam, Elsevier 1988.
[13] SKLENIČKA, V.—KUCHAŘOVÁ, K.—DLOUHÝ, A.—KREJČÍ, J.: In: Proc. Conference on Materials for Advanced Power Engineering. Eds.: Coutsoudaris, D. et al. Dordrecht, Kluwer Academic Publishing 1994, p. 435.
[14] ČADEK, J.—ŠUSTEK, V.—PAHUTOVÁ, M.: Mater. Sci. Eng., *A225*, 1997, p. 22.
[15] ORLOVÁ, A.—BURŠÍK, J.—KUCHAŘOVÁ, K.—SKLENIČKA, V.: Mater. Sci. Eng., *A245*, 1998, p. 39.
[16] RÖSLER, J.—ARZT, E.: Acta Metall. Mater., *38*, 1990, p. 671.
[17] KUCHAŘOVÁ, K.—NĚMEC, J.—DLOUHÝ, A.: In: Proceedings of the Int. Conference on Creep and Fracture of Engineering Materials and Structures. Eds.: Earthman, J. C., Mohamed F. A. Irvine, University Press Irvine 1997, p. 79.
[18] ENNIS, J. P.: see [1], p. 187.
[19] HATTESTRAND, M.—ANDREN, H.-O.: Micron, *32*, 2001, p. 789.
[20] HALD, J.: see [1], p. 115.